Structural dynamics of a colloidal protein-mineral complex bestowing on calcium phosphate a high solubility in biological fluids

A. Heiss[a] and W. Jahnen-Dechent
Institute for Biomedical Engineering, Biointerface Group, RWTH Aachen University, Pauwelsstrasse 30, D-52074 Aachen, Germany

H. Endo and D. Schwahn[b]
Institute for Solid State Research, Research Center Jülich, D-52425 Jülich, Germany

(Received 12 January 2007; accepted 13 February 2007; published 29 March 2007)

The concentration of mineral solutes in mammalian blood is considerably higher than that predicted by their solubility product. The plasma protein fetuin-A inhibits calcium phosphate deposition by forming colloidal calciprotein particles (CPPs). In this article the authors present a detailed *small angle neutron scattering* study including contrast variation analysis providing detailed quantitative information on the three-dimensional topology of the CPPs and on their morphogenesis. In detail the authors found the following: (i) A two stage growth process showing spontaneously formed primary particles with a size of about 500 Å diameter that subsequently transformed to 1000 Å sized particles which were stable for at least 24 h. (ii) A particular shielding topology was observed for the second CPP state, namely, that a densely packed fetuin-A monolayer covers a mineral core and thereby prevents further crystal growth. (iii) Transmission electron microscopy analysis of *in vitro* synthesized second state CPPs revealed striking similarities to material retrieved from a human peritonitis patient. This latter finding underscores the importance of short- and long-term stabilizations of CPPs by fetuin-A to enable clearing of mineral debris in the body. © *2007 American Vacuum Society.* [DOI: 10.1116/1.2714924]

I. INTRODUCTION

Thermodynamics predict that many biological fluids including blood should precipitate solid minerals because of solute supersaturation. This is, however, not the case. Therefore inhibitory principles are claimed to prevent the formation and buildup of insoluble minerals. Genetic studies using knockout mice identified the serum protein fetuin-A/α_2-HS glycoprotein as an important inhibitor preventing pathological mineralization in soft tissues and in the extracellular fluid.[1] Dialysis patients are prone to vascular and valvular calcifications and have severely reduced fetuin-A serum levels, likewise suggesting an important role of fetuin-A in the prevention of pathological mineralization.[2] A transmission electron microscopy (TEM) and dynamic light scattering (DLS) study identified calciprotein particles (CPPs), i.e., colloidal nanoparticles of fetuin-A, calcium, and phosphate as the entities solubilizing calcium phosphate mineral. Furthermore, the TEM analysis showed that CPPs are initially amorphous but subsequently transform in size and morphology due to crystallization.[3] A study measuring ionized calcium during CPP transformation likewise reported a stepwise decrease in the calcium concentration providing further evidence of a staged ripening of the mineral nuclei in the presence of fetuin-A.[4]

The stability and size of the CPP colloids have thus been determined independently by us and others,[3,4] but the molecular topology is still unknown. Here we present a detailed *small angle neutron scattering* (SANS) study including contrast variation analysis to provide detailed quantitative information on the three-dimensional topology of the CPPs and on their morphogenesis. In detail we determined the following: (i) a two step growth process showing rapid formation of primary particles with a size of about 500 Å diameter that subsequently transformed to 1000 Å sized particles which were stable for at least 24 h. (ii) The morphology of the second stage particles consisted of a mineral core covered by a protein shell. (iii) The structure determined by SANS experiments closely matched TEM images of CPPs isolated from ascites fluid of a dialysis patient suffering from calcifying peritonitis.

II. METHODS

A. CPP synthesis

Bovine fetuin-A monomer was isolated from a commercial preparation (Sigma) by size exclusion chromatography using a Superdex 200 16/60 column (GE Healthcare). All SANS experiments described below were performed at final concentrations of 2.5 mg/ml bovine fetuin-A, 10 mM $CaCl_2$, 6 mM Na_2HPO_4, 140 mM NaCl, and 50 mM tris-HCl *p*H7.4 (obtained from Merck, Darmstadt and Roth, Karlsruhe, Germany, all at analytical quality).

B. Small angle neutron scattering

The SANS experiments were performed at the FRJ-2 research reactor of the Research Center-Jülich (Germany).[5] Neutron lenses were installed in order to achieve a higher

[a]Electronic mail: alexander.heiss@post.rwth-aachen.de
[b]Electronic mail: d.schwahn@fz-juelich.de

TABLE I. Physical properties of CPP components. Density and size of fetuin-A were assessed by ultracentrifugation; the scattering length density ρ was obtained from SANS experiments. The ρ for HAP and OCP were evaluated considering the corresponding mass densities taken from Ref. 11. ϕ represents the D_2O concentration in solution.

	Water	Fetuin-A	Hydroxyapatite	OCP
Density (g/ml)	1	1.317	3.2	2.61
Molar weight	⋯	50 kDa	1.004 kg/mol	0.983 kg/mol
Chemical formula	$D_2O[\phi]+H_2O[1-\phi]$	⋯	$Ca_{10}(PO_4)_6(OH)_2$	$Ca_8H_2(PO_4)_6$ $5(H_2O)$
$\rho(10^{10}\ \mathrm{cm}^2)$	$-0.561+6.951\phi$	$1.46+1.95\phi$	$4.26+0.4\phi$	$3.07+1.99\phi$

neutron flux. The SANS signal is expressed by the macroscopic cross-section $d\Sigma/d\Omega$ and is measured as a function of the wave vector $Q=(4\pi/\lambda)\sin(\delta/2)$ (λ neutron wavelength and δ scattering angle). For composite particles as protein-mineral colloids $d\Sigma/d\Omega$ can be separated into partial scattering functions according to

$$\frac{d\Sigma}{d\Omega}(Q) = (\rho_M - \rho_W)^2 P_{M,M}(Q) + (\rho_P - \rho_W)^2 P_{P,P}(Q) + 2(\rho_M - \rho_W)(\rho_P - \rho_W) P_{P,M}(Q). \quad (1)$$

The subscripts M, W, and P refer to mineral, water, and protein, respectively. The relative contribution of the individual partial scattering functions, $P_{i,j}$, depends on the scattering contrast $(\rho_i-\rho_W)^2$, i.e., the square of the difference of the coherent scattering length density of component i and the solvent water (W). The scattering length density of a molecule is defined by $\rho=\Sigma c_j b_j/\omega$ (b_j coherent scattering length, c_j concentration of atom j, and ω the corresponding filled volume). Contrast variation takes advantage of the strongly different coherent scattering lengths of hydrogen $b_H=-3.7423\times10^{-13}$ cm and deuterium $b_D=6.674\times10^{-13}$ cm. By adjusting the scattering length density of the solvent (ρ_W) through D_2O content, the scattering length density of a protein component (ρ_P) or a mineral component (ρ_M) can be matched so that it no longer contributes to the scattering, i.e., $\rho_W=\rho_i$. In principle the self-terms could be obtained by adjusting $\rho_W=\rho_P$ or $\rho_W=\rho_M$. However, Eq. (1) shows that this is not possible for the cross term. Distinct scattering length densities (ρ_P and ρ_M) are required to study the two CPP components protein and mineral separately. These scattering length densities were determined unambiguously showing their matching point at 40.4% (protein) and 73% (mineral) D_2O content, respectively. The scattering length densities of all components given in Table I slightly change with the concentration of D_2O due to the hydrogen content of the mineral as well as the H/D exchange on the surface of the protein.[6]

The partial scattering functions are expressed as $\mathbf{P}(Q)=[\mathbf{\Delta\rho}^2]^{-1}\mathbf{I}(Q)$. Here the vectors $\mathbf{I}(Q)=\{d\Sigma/d\Omega(Q)_k\}$ and $\mathbf{P}(Q)=\{P_{i,j}(Q)\}$ represent the scattering intensities from an experimental series and the partial scattering functions, respectively, whereas the matrix $[\mathbf{\Delta\rho}^2]=[\{\rho_i-\rho_k\}\{\rho_j-\rho_k\}]$ represents the contrasts of protein and/or mineral with respect to water. The type of matrix and the dimension of the vectors depend on the number k of measured contrasts and the number of independent partial scattering functions $i,j=\{M,P\}$ (i and j could be either M or P). The determination of the "pseudo inverse" of the matrix $[\mathbf{\Delta\rho}^2]$ is a basic mathematical procedure, which was performed using the method of "singular value decomposition" as the matrix is usually not of a quadratic nature.[7] In order to determine $\mathbf{P}(Q)$, a set of samples with identical mineral ion and fetuin-A content but varying H_2O/D_2O ratios was measured using SANS. Our calculations were based on an overdetermined set of equations, i.e., the number of measured contrasts is larger than the number of independent partial scattering functions, in order to improve the reliability of the extracted partial scattering functions.

Relying on classical SANS theory, the self-terms were further analyzed according to

$$P(Q) = P(0)\exp(-u^2/3) + p_\alpha[(\mathrm{erf}(u\sqrt{6}))^3/Q], \quad (2)$$

which combines the approximate laws at low (Guinier's law) and large Q (Porod's law) with $u=(R_gQ)$ and R_g (radius of gyration).[8] With regard to the data presented here, a $\alpha=4$ represents compact particles with a sharp interface S, i.e., $p_4=2\pi nS$.

C. Transmission electron microscopy

50 μl of CPP solution prepared *in vitro* or isolated from patient ascites were dialyzed in mini Slide-A Lyzers (Pierce) against distilled water (1:10 000) for 20 min at room temperature. 5 μl solution was applied onto copper-carbon grids (Plano, Wetzlar, Germany). After incubation for a few minutes, excess solution on the grid was removed. The samples were examined in the TEM, JEOL JEM 2000 FX II and Philips EM 400 T/ST, operated at 200 kV without staining.

III. RESULTS AND DISCUSSION

Fetuin-A is a unique protein inhibitor of calcification in that it acts on the systemic level in all extracellular spaces. Acidic serum proteins in general may also interfere with spontaneous calcium phosphate precipitation when tested *in vitro*. The most abundant serum protein, serum albumin, is however, a relatively weak inhibitor of calcium phosphate precipitation, i.e., at a concentration 100-fold higher than fetuin-A, and only short term.[9] This renders serum albumin

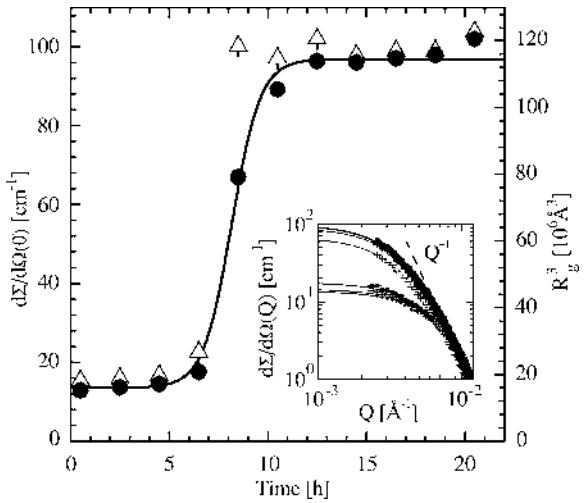

FIG. 1. Time dependency of the volume (-Δ-) and the volume multiplied by the volume fraction (-●-) of the CPPs expressed as R_g^3 (-Δ-) and the extrapolated cross section at $Q=0$, $d\Sigma/d\Omega(0)$, (-●-) vs mineralization time. The plot of the CPP sample in 100% H_2O revealed a two stage mineralization process with plateaus at 0–5 and 11–20 h. The inset shows the corresponding scattering patterns. These data were fitted according to Eq. (2), depicted by the solid lines.

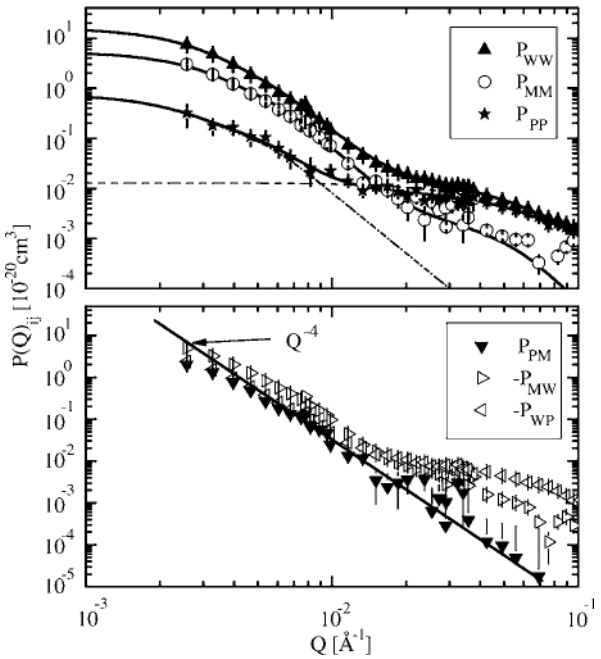

FIG. 2. Partial structure functions derived from $d\Sigma/d\Omega$ of six identical CPP samples with varying H_2O/D_2O content. These data are not shown here. The self-terms of water (W), mineral (M), and protein (P) are plotted in the upper graph and the corresponding cross terms in the lower graph. The positive cross-term $P_{P,M}$ suggested a protein covered mineral core.

an ideal control protein for the study of calcium phosphate precipitation inhibition by fetuin-A. We measured bovine serum albumin (0.66 mg/ml) in scattering measurements at 5 mM $CaCl_2$ and 2 mM Na_2HPO_4.[10] As already reported for serum albumin inhibition of precipitation by radioactive pellet measurements[3,9] we observed faster particle growth in the presence of albumin than of fetuin-A. High mineral ion supersaturation (10 mM $CaCl_2$ and 6 mM Na_2HPO_4) was required to obtain sufficient scattering intensity. At this mineral supersaturation albumin even at concentrations up to 40 mg/ml never mediated any soluble particle formation beyond a few minutes precluding SANS experiments for a detailed structural analysis. Hence we only report on SANS data obtained with fetuin-A.

Physicochemical data on the characteristics of the individual components are listed in Table I. Values were either derived from analytical ultracentrifugation for fetuin-A or were taken from textbook references for HAP and octacalcium phosphate (OCP).[11] Figure 1 shows a kinetic experiment with time dependent extrapolated scattering at $Q=0$ and R_g^3; both parameters were derived from fits of Eq. (2) depicted as solid lines in the inset of Fig. 1. Guinier's as well as Porod's Q^{-4} regimes fit well within their respective Q regimes, indicating compact particles. The mineralization process was monitored for 21 h and intermediates were analyzed by SANS with 1 h data sampling periods for each data point. The SANS measurements clearly indicated a two step transformation of CPPs. The initial sample contained the fetuin-A monomer with a $R_g=30\pm1$ Å, which is in agreement with our previous light scattering measurements $R_g=32$ Å.[3] Particles of $R_g=260$ Å formed spontaneously upon calcium and phosphate mixing. After about 5 h of incubation a slow transition to a second stationary stage occurred which was completed within another 5 h. The particles representing the second stage showed an average radius of gyration of $R_g=490$ Å and were stable for the remaining duration of exploration (21 h).

The second stage of fetuin-A induced mineral stabilization most likely represented the final CPP state before sedimentation occurred. This CPP structure was further explored by SANS with contrast variation. The corresponding self-terms of the mineral $P_{M,M}(Q)$ and the protein $P_{P,P}(Q)$, as the cross term of the protein-mineral $P_{P,M}(Q)$, are shown in Fig. 2. These data were derived from measurements of six identical CPP samples with varying H_2O/D_2O ratios. In addition we derived the water self-term $P_{W,W}(Q)$, the mineral-water $P_{M,W}(Q)$, and protein-water $P_{P,W}(Q)$ cross terms as well. $P_{W,W}(Q)$ was derived on the basis of *Babinet's principle* for incompressible systems, i.e., scattering from density fluctuations is negligible, stating that the self-term of water is equal to the coherent superposition of the scattering resulting from protein and mineral according to $P_{W,W}=P_{M,M}+P_{P,P}+2P_{P,M}$.[7,12] Hence $P_{W,W}(Q)$ can be considered as scattering from "voids" in water which are, in fact, comprised of CPP and protein monomers.

From $P_{W,W}(Q)$ at low Q we calculated a radius of gyration of $R_{g,\mathrm{CPP}}=615\pm32$ Å for the entire CPP. Likewise we assessed the size of the CPP's mineral and protein phases $R_{g,M}=566\pm61$ Å and $R_{g,P}=685\pm49$ Å from $P_{M,M}(Q)$ and $P_{P,P}(Q)$, respectively. The smaller radius of gyration for the mineral phase, i.e., $R_{g,M}<R_{g,W}$, as well as the larger $R_{g,P}>R_{g,W}$ indicated the presence of a mineral core covered by a fetuin-A layer. Assuming a compact protein layer, a radius of gyration of $R_{g,P}=765\pm84$ Å was deduced from the measured

$R_{g,M}$ and $R_{g,W}$, which is fully consistent with the values previously measured by TEM and DLS. Furthermore, a sharp mineral interface was indicated by the $P_{M,M} \propto Q^{-4}$ Porod behavior. Please note that P_{WW} suggested a 20% larger R_g for the CPPs than $d\Sigma/d\Omega$ in Fig. 1. This variance resulted from the lower scattering contrast of the fetuin-A layer compared to the mineral core in H_2O solution which is relevant for $d\Sigma/d\Omega$ but not for P_{WW}.

Further evidence supporting a model of a mineral core covered by a fetuin-A layer was derived from the protein-mineral cross-term $P_{P,M}$. This cross term is related to the self-terms according to $[P_{W,W}(Q) - P_{M,M}(Q) - P_{P,P}(Q)]/2$. At $Q=0$ the cross term is always positive according to $P_{p,M}(0) = n_M V_M V_P$ which was obtained from entering the self-terms $P_{i,i}(0) = n_i V_i^2$ (n_i number density and V_i volume). However, at Q larger than the inverse size of the mineral particle the cross-term $P_{P,M}$ provides information on the relative spatial arrangement of protein and mineral within the CPPs. In two alternative CPP models, namely, (i) a homogeneous distribution of proteins inside or (ii) a protein layer on the outside of the mineral, the cross term should differ by a negative contribution of the protein self-term. Thus, (i) $P_{P,M} \cong -P_{P,P}$ (for $R_g \cong 500$ Å particles at about $Q > 10^{-2}$ Å^{-1}) would indicate that fetuin-A is enclosed within the mineral phase, whereas (ii) $P_{P,M} \geqslant 0$ would indicate that fetuin-A is attached to the surface of a mineral core. Figure 2 shows that the cross-term $P_{P,M}(Q)$ was positive only, in particular, above $Q > 10^{-2}$ Å^{-1}, suggesting the structure of a protein-free mineral core covered by a fetuin-A layer mediating complex solvation in water. From the invariant $Q2 = \int Q^2 P(Q) dQ \cong 2\pi^2 \Phi$ and $P(Q=0)$ we determined a protein volume fraction of the CPPs between 20% and 25% corresponding to 3% of the total fetuin-A present in the reaction mixture.[12] Calculations based on the fetuin-A volume fraction and the radii within the CPP thus suggested a compact monolayer.

The contrast variation experiments suggested that OCP and not hydroxyapatite was the mineral polymorph in second state CPPs. Entering the scattering length density of hydroxyapatite into the matrix calculations [Eq. (1)] would result in $P_{P,M}(Q) > P_{M,M}(Q)$, implying a larger volume for the attached proteins than the mineral, which clearly contradicts the chemical composition. On the basis of an OCP polymorph, we assessed from the invariant $Q2$ a mineral volume fraction of 2×10^{-4}, suggesting that the mineral core comprised 60% of all mineral ions originally present in the precipitation mix. This value corroborated a biochemical study estimating the residual ionic calcium concentration under similar mineralization conditions.[4]

The morphology of the second state CPPs was also studied by TEM analyses. SANS and TEM ideally complement each other as TEM visualizes individual particles whereas SANS delivers averaged quantitative data of particles dissolved within a volume of the order 0.1 ml. Figure 3(a) depicts representative CPPs of the second state, revealing a spheroid morphology with the two shorter and larger semiaxes of roughly $a=500$ Å and $b=1000$ Å, respectively ($v=b/a$). According to $R_g = a\sqrt{(2+v^2)/5}$ we calculate a radius of gyration of $R_g = 550$ Å which is consistent with the SANS data.[12]

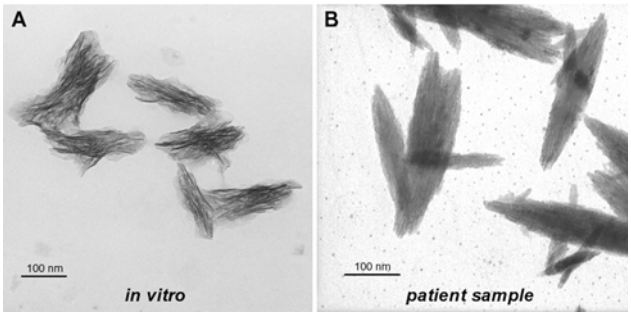

FIG. 3. TEM images of protein-calcium phosphate mineral colloids. (A) *In vitro* sample of a CPP in the second state generated under the same conditions of the SANS experiments (10 mM $CaCl_2$, 6 mM Na_2HPO_4, 50 mM tris-HCl and 140 mM NaCl). (B) Peritoneal dialysate of a dialysis patient containing protein-calcium phosphate particles closely resembling the CPPs generated *in vitro* and shown in (A).

Figure 3(b) shows a TEM image of a sample from a human patient with calcifying peritonitis. This side by side comparison revealed striking similarities between the *in vitro* synthesized second state CPPs and the patient sample. Both samples contained elongated spheroidal structures of similar size and crystallinity. This result suggested that long-term stabilization of second state CPPs may be equally important like short-term inhibition of spontaneous calcium phosphate precipitation in the overall inhibition of pathological mineralization. The high density fetuin-A monolayer on the second state CPP surface is intriguing in that it suggests a putative CPP clearing mechanism. We hypothesize that the putative CPP clearing mechanism relies on the cellular recognition of clustered fetuin-A. This kind of molecular recognition by phagocytic cell receptors would efficiently discriminate against the excess monomeric fetuin-A in the extracellular fluid, which would otherwise compete with CPP uptake. Conversion of low affinity to high affinity recognition by ligand clustering is, in fact, common in clearing of cellular debris and particles, but has never been suggested for clearing of mineralized debris.

In summary, we demonstrated that SANS ideally lends itself to a study of protein-mineral interaction in biomineralization research. This method does not denature biological samples, it covers the relevant size range between 10 and 1000 Å and reveals both internal structure and composition. The SANS analysis employed here revealed the dynamic transformation of CPPs into a layered colloid comprising an OCP core and a fetuin-A shell. Thus we provide experimental proof of a hitherto theoretical concept of a protein shielding mechanism preventing pathological mineralization.[4,13,14] In addition the core-shell structure suggests strongly reduced diffusion of ions across the colloid mineral interface resulting in a reduced CPP growth and OCP to HAP transformation. The structure of CPPs prepared *in vitro* closely resembled TEM pictures of CPP samples from a human patient suffering from calcifying peritonitis, adding strong clinical

relevance to our structural analysis. In conclusion, this detailed description of CPP morphology may aid the rational design of clinical assays of pathological mineralization risk and of synthetic inhibitors alike.

ACKNOWLEDGMENTS

The authors thank Helmut Cölfen (Max-Planck-Institute of Colloids and Interfaces, Golm, Germany) for ultracentrifugation analysis, Sven Brincker for excellent technical assistance, Anke Aretz and Manfred Bovi (all RWTH Aachen University) for TEM imaging, Manfred Heiderich for excellent technical assistance, and Dieter Richter (both Research Center Jülich, Germany) for helpful discussions. Patient samples were provided by Wim van Dorp (Haarlem, Netherlands). This study was supported by the Deutsche Forschungsgemeinschaft within the priority program "Principles of Biomineralization" (A.H., W.J.D., and D.S.).

[1]C. Schäfer *et al.*, J. Clin. Invest. **112**, 357 (2003).
[2]M. Ketteler *et al.*, Lancet **361**, 827 (2003).
[3]A. Heiss, A. DuChesne, B. Denecke, J. Grötzinger, K. Yamamoto, T. Renné, and W. Jahnen-Dechent, J. Biol. Chem. **278**, 13333 (2003).
[4]P. A. Price and J. E. Lim, J. Biol. Chem. **278**, 22144 (2003).
[5]http://www.fz-juelich.de/iff/wns_kws1
[6]G. Zaccai, J. Phys. Chem. Solids **60**, 1291 (1999).
[7]H. Endo, D. Schwahn, and H. Cölfen, J. Chem. Phys. **120**, 9410 (2004).
[8]G. Beaucage, J. Appl. Crystallogr. **29**, 134 (1996).
[9]T. Schinke, C. Amendt, A. Trindl, O. Pöschke, W. Müller-Esterl, and W. Jahnen-Dechent, J. Biol. Chem. **271**, 20789 (1996).
[10]A. Heiss and D. Schwahn, in *Handbook of Biomineralization* (Wiley-VCH, Weinheim, Germany, 2007), Vol. 1, pp. 415–431.
[11]J. C. Elliot, *Structure and Chemistry of the Apatites and Other Calcium Orthophosphates* (Elsevier Science, Amsterdam, 1994).
[12]J. S. Higgins and H. C. Benoit, *Polymers and Neutron Scattering* (Clarendon, Oxford, 1994, pp. 116–191.
[13]N. C. Blumenthal, F. Betts, and A. S. Posner, Calcif. Tissue Res. **18**, 81 (1975).
[14]L. Addadi and S. Weiner, Proc. Natl. Acad. Sci. U.S.A. **82**, 4110 (1985).